Robust MPC Tower Damping for Variable Speed Wind Turbines

Martin A. Evans, Mark Cannon, and Basil Kouvaritakis

***Abstract*— Model predictive control (MPC) is receiving attention in wind turbine controller design due to its ability to explicitly handle state and input constraints. Robust model predictive control (RMPC) additionally accounts for uncertainty in the future evolution of the system. Here, RMPC is compared with nominal MPC for the purposes of fore-aft tower damping of large wind turbines. The two controllers are identical save for their handling of the multiplicative and additive uncertainty in the prediction horizon. The comparison is performed by means of fatigue analysis in a state-of-the-art aeroelastic simulation package. State and input constraints are applied to a control model that is identified by data-driven methods. The robust controller bounds the uncertainty with a sequence of polytopes, which tighten the constraints to reduce constraint violations, while retaining the computational complexity of a quadratic program.**

***Index Terms*— Active damping, model predictive control (MPC), robust control, wind turbines.**

I. Introduction

LARGE wind turbines suffer fatigue damage to the tower due to fore-aft motion driven by aerodynamic thrust. Structural mitigation of this adds significantly to the material cost of the machine. Passive dampers have been used [1] to reduce tower fatigue, such as pendula in oil, but these are expensive and must be tuned to a single frequency despite their sensitivity to ambient temperature and the rotor's sensitivity to wind speed.

Active control of the rotor thrust is an attractive alternative approach. A thorough review of control methods for variable speed turbines is given in [2], including active damping of the first fore-aft tower mode. Rotor thrust control can be achieved by varying the blade pitch angle, which is normally used only to control the rotor speed. Gain scheduling is shown to be important due to the wide variation of pitch sensitivity with wind speed. Coupling between pitch control for tower damping and pitch control for rotor speed above the rated wind speed motivates a multivariable control approach. An linear parameter varying (LPV) approach covering the entire operating wind speed range is found in [3].

Model predictive control is a near-optimal control method that uses online computation to address multivariable control problems subject to input and state constraints. A detailed review of MPC for constrained systems is found in [4]. As quadratic programming (QP) solvers become more advanced, MPC is becoming an attractive method of control of wind turbines that have constraints, such as the stall pitch angle (where pitch angles too low for the rotor speed and wind speed cause the rotor blades to stall), maximum rotor speed, and maximum power.

Early work that aimed at controlling a wind turbine with predictive control [5] did so without constraints. The predictive element of MPC has often required the estimation of future wind speeds. In [6], this was estimated from past wind speeds, giving modest performance predicting wind speed in the very short-term future. In modern turbines, there is the potential for wind speed feedforward with light detection and ranging, or lidar, a technology for measuring the wind speed upstream of the rotor [7]. Lidar systems cannot fully measure the future wind speeds, so recent work explicitly accounts for uncertainty in the prediction horizon, and handles constraints robustly, as in [8]. This brief does not assume that any preview signal is available.

Many prior works have applied linear MPC to a wind turbine by restricting the control model to a single operating point. However, linear models of a wind turbine depend greatly on wind speed, and this identifies a need for a control scheme that covers the whole range of wind speeds. Early works to do so were [9] and [10]. Both handle uncertainty in the future wind speed using multiple models optimized separately online, switched or mixed on the basis of a filtered wind speed scheduling signal to arrive at the control action. In [11], a hybrid MPC structure is proposed to handle switching between operating modes. The results therein show using a high-fidelity aeroelastic code that MPC can handle constraints more favorably than anti-windup proportional-integral (PI) control.

A multiple-model MPC, such as [9] and [10], has a drawback that while each model can be optimized for a different wind speed, the predictions for that model assume constant wind speed throughout the horizon. In reality, the wind speed will vary significantly during the prediction horizon. The present robust model predictive control (RMPC) controller allows for a range of possible wind speeds in the prediction horizon by bounding the set of uncertain state predictions by polytopes for the purposes of enforcing state and input constraints. This allows for uncertainty in both the state transition matrix and the input gain matrix, whereas previous work on RMPC in the context of wind turbine control, such as [8] and [12], has restricted this uncertainty to the latter for ease of derivation of an optimization method. A formulation of the uncertainty bounds in the prediction horizon that results in a quadratic program to solve is given in [13]. This brief in part constitutes an application of this method to an LPV system.

Manuscript received October 15, 2013; revised February 26, 2014; accepted March 4, 2014. Manuscript received in final form March 6, 2014. This work was supported in part by Vestas Technology U.K. Ltd., and in part by the Engineering and Physical Sciences Research Council. Recommended by Associate Editor E. Kerrigan.

The authors are with the Department of Engineering Science, University of Oxford, Oxford OX1 3JP, U.K. (e-mail: martin.evans@eng.ox.ac.uk; mark.cannon@eng.ox.ac.uk; basil.kouvaritakis@eng.ox.ac.uk).

Color versions of one or more of the figures in this paper are available online at http://ieeexplore.ieee.org.

Digital Object Identifier 10.1109/TCST.2014.2310513

RMPC requires a model of the controlled plant that must contain reasonably accurate bounds on the distributions of uncertain parameters and exogenous inputs. This brief derives a simple piecewise linear model whose matrix elements are functions of wind speed. These functions are estimated in a straightforward manner by offline data-driven methods. A more rigorous approach to data-driven model identification is given in [14, Sec. III]. The MPC controllers we present can easily be applied to models identified by more advanced techniques that are outside the scope of this brief.

This brief is organized as follows. Section II gives the nonlinear dynamic equations that govern pitch-regulated wind turbines. Section III gives a method of finding a linear model that is suitable for operation at a given mean wind speed, and explains how a set of these models can be interpolated for operation at any wind speed. Section IV shows how the uncertainty that enters the prediction horizon due to model uncertainty and unknown wind speeds can be handled by an RMPC strategy that uses polytopes to bound uncertainty in the evolution of the model state. Section V derives a quadratic cost function based on expectations to be minimized online. The predictive control model has parameters that are found by simple numerical model identification. The methods we use for this identification are given in Section VI. Finally, the nominal and robust algorithms are compared in Section VII by numerical simulations, followed by some concluding remarks.

The novel contributions of this brief are the application to the wind turbine control problem of a robust MPC scheme that handles multiplicative and additive uncertainty while posing an easily solved quadratic program, and the tower loads comparison of the resulting controller against nominal MPC.

II. Nonlinear Dynamics

This section gives an overview of wind turbine dynamics as a context into which the control model of Section III is introduced. The aeroelastic simulation environment in which the resulting controller is tested does not have the following simplifications applied. Details of that simulation environment are given in Section VII. The control model assumes rigid rotor blades, rigid drivetrain, negligible generator and pitch system dynamics, and no pitch-induced dynamic lift. A standard wind turbine model [3] incorporating the out-of-plane thrust on the rotor, mechanical power in the rotor and electrical power in the generator, and a lumped-parameter model of tower bending is thus summarized. The symbols and parameters are explained in Table I.

A wind turbine derives its rotational mechanical power from the in-plane component of lift as air flows over the surfaces of the rotor blades, as a result of the combined action of the normal component of wind velocity and the rotation of the rotor. The lift forces depend on the pitch angle of the rotor blades, the rotor speed, and the wind speed. Generator speed is assumed proportional to rotor speed due to the rigid drivetrain

$$P_a = \frac{1}{2} a \rho v^3 c_P(\beta, \lambda) = Q_a \Omega. \tag{1}$$

The out-of-plane component is thrust, a force applied at the tower top. The tower can be considered a lightly damped flexible beam. The motion of the rotor disk into the wind changes the thrust, which introduces damping that varies significantly with wind speed

$$F_T = \frac{1}{2} a \rho v^2 c_T(\beta, \lambda) = \kappa p + \gamma(v)\dot{p} + m\ddot{p}. \tag{2}$$

Power is extracted from the turbine by a generator, connected via the drivetrain (including a gearbox) to the rotor

$$P_a - P_e = \Omega(Q_a - Q_e) = \Omega \dot{\Omega} J = \frac{1}{2} \frac{d\Omega^2}{dt} J. \tag{3}$$

In the absence of constraints on the generator power, controlling the rotor speed would be a trivial case of matching generator power to aerodynamic power. This is indeed the case when the wind speed is below rated, a situation termed partial load. However, the above-rated wind speed and aerodynamic power must be reduced by pitching into a less efficient angle of attack, termed full load. This brief presents a controller that respects the underlying constraints rather than treating these two operating modes separately.

TABLE I
Nonlinear Model Parameters

P_a	Mechanical rotor power
a	Rotor area
ρ	Air density
v	Wind speed (averaged over the rotor disk)
c_P	Coefficient of power
β	Pitch angle
λ	Tip speed ratio $\propto \Omega/v$
F_T	Thrust acting on tower downwind
c_T	Coefficient of thrust
κ, γ, m	Lumped parameter tower stiffness, damping, mass
p	Tower top displacement fore-aft
J	Rotor+drivetrain+generator inertia
Q_a	Rotational torque at rotor
Q_e, P_e	Torque at generator, generator power
Ω	Rotor speed

III. Control Model

For the purposes of controller design, we adapt (1)–(3) to construct a state-space model with state $x_k \in \mathbb{R}^{n_x}$ at time step k comprising fore-aft tower displacement p, fore-aft velocity $\dot{p}$, and rotor speed squared Ω^2. The square of the rotor speed is used to provide a linear relationship with electrical power. The vector $u_k \in \mathbb{R}^{n_u}$ of input variables to be specified by the controller at time step k comprises pitch angle β and generator power P_e. The dynamics are approximated so as to evolve the state according to the LPV difference equation

$$x_{k+1} = A(v_k)x_k + B(v_k)u_k + w(v_k) \tag{4}$$

where matrices $A(v)$, $B(v)$, and $w(v)$, which depend explicitly on wind speed v, are obtained by data methods based on time series taken from closed-loop operation under an existing controller in the aeroelastic simulation environment and are treated piecewise linear in v.

The constraints considered are the following: the blades must not stall or exceed 90°; the squared rotor speed, as a ratio of the squared nominal rotor speed for a given wind speed $\bar{\Omega}^2(v)$, must lie within a fixed interval, e.g., $[m^-, m^+] = [0.75, 1.25]$; and the generator power must lie between zero

and nominal, $\bar{P}_e$. For a given wind speed and rotor speed, there is a known stall angle $\beta^s(v,\Omega)$, which the pitch angle must exceed. For a given wind speed, there is a known optimum rotor speed. The nominal rotor speed is the smaller of this optimum and a limit imposed by the turbine design. Rate constraints could easily be incorporated

$$\begin{bmatrix}\beta^s(v,\Omega)\\ 0\end{bmatrix} \le u \le \begin{bmatrix}90\\ \bar{P}_e\end{bmatrix} \tag{5a}$$

$$\bar{\Omega}^2(v)m^- \le \Omega^2 \le \bar{\Omega}^2(v)m^+ \tag{5b}$$

$$Fx + Gu \le g(v). \tag{6}$$

The constraints of (5) are more usefully written in the form of (6). Although this is time varying, mild assumptions allow us to treat $g(v)$ as constant over the MPC prediction horizon. We minimize an infinite horizon cost, as given in Section V. Predictions are made N steps ahead of the present state, with an assumption of perfect measurements, although measurement uncertainty can be easily incorporated in the setup described here.

Control model identification is performed around wind speeds in the discrete set $\mathcal{V}$ to give the model set $\{\hat{A}(v) : v \in \mathcal{V}\}$. Values of $A(v)$ between these wind speeds are linearly interpolated. Functions $B(v)$ and $w(v)$ are defined analogously in terms of $\mathcal{V}$. Section VI discusses model identification, where derivations of the values for these functions are given.

The selection of the scheduling parameter would ideally be the mean wind speed over the rotor area. However, an anemometer wind measurement taken atop the nacelle cannot measure this. Turbulent wind at the height at which large turbines operate typically has a length scale similar to the diameter of the rotor [15], so filtering the anemometer signal with a sufficiently long time constant gives a simple estimation, $\tilde{v}$, of the spatial average of the wind speeds across the rotor area over that time. The time constant we use for this filter in the numerical examples is 5 s, chosen to be fast enough to respond to gusts but slow enough to provide some element of spatial wind estimation. Alternatively, a wind speed estimator could be used for the scheduling parameter, such as in [12]. We opted for a filter for simplicity.

IV. Robust Control Design

The control model is uncertain due to future wind speeds being uncertain and model-plant mismatch. The approximation error in the control model for any given wind speed, i.e., the difference between the dynamics of (1)–(3) and (4) is subsumed into the uncertainty on the additive term $w(\tilde{v})$. The predicted filtered wind speed at time step $k+i$, denoted by $v_{i|k}$, is assumed to lie in the range $[v^-_{i|k}, v^+_{i|k}]$. Large ranges lead to conservative operation, while small ranges increase the chance that the wind will exceed the assumed bounds, potentially leading to infeasibility. A suitable formulation for the bounds is given in (7), where τ is a constant defining the exponential rate at which the uncertainty builds over the horizon and n_c is the number of standard deviations σ of the wind speed above and below $\tilde{v}_k$ to include

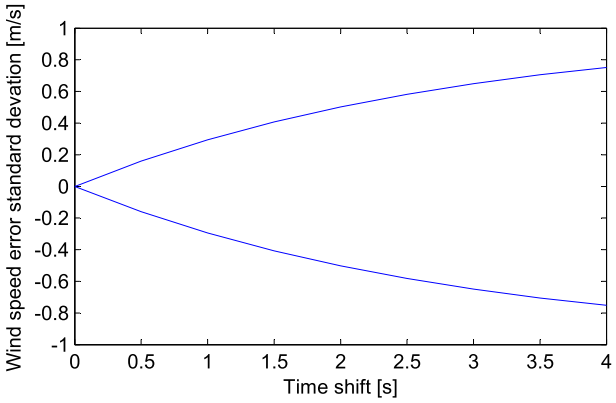

Fig. 1. Characterizing the wind speed uncertainty in the prediction horizon. From 600 s of filtered wind speed $\tilde{v}(t)$, we create eight time series $\tilde{v}(t) - \tilde{v}(t + i\Delta t)$, $i = 1,\ldots,8$, $\Delta t = 0.5$. This figure shows ± 1 standard deviation of each of these series. Fitting (7) to this, we find $\tau = 0.84$. In this example, the mean wind speed was 10 m/s with 10% turbulence intensity.

$$v^{\pm}_{i|k} = \tilde{v}_k \pm n_c\sigma(1-\tau^i). \tag{7}$$

Suitable values for these parameters can be found by analyzing wind time series, as shown in Fig. 1, or by simulation, such as in [8, Sec. IV]. For nominal MPC operation, $n_c = 0$.

Since the cost to be discussed in Section V has the form of an expectation over stochastic parameters, we must approximate the probability distribution of the wind speeds within the range given by (7). Specialized studies into the statistics of the wind turbulence could be used to produce an ideal distribution for this purpose, but for simplicity, we instead use the triangular distribution

$$f(v_{i|k}|\tilde{v}_k, r) = \begin{cases}(r - |v_{i|k} - \tilde{v}_k|)/r^2 & : \quad |v_{i|k} - \tilde{v}_k| < r\\ 0 & : \quad \text{otherwise}\end{cases} \tag{8}$$

where $r = n_c\sigma(1-\tau^i)$.

The uncertain dynamics are

$$x_{i+1|k} = \left(A^0_k + A^\delta_{i|k}\right)x_{i|k} + \left(B^0_k + B^\delta_{i|k}\right)u_{i|k} + \left(w^0_k + w^\delta_{i|k}\right) \tag{9}$$

where superscript zero denotes nominal, e.g., $A^0_k = A(\tilde{v}_k)$, and superscript δ denotes uncertainty, with $A^\delta_{i|k}$ assumed to belong to a polytopic set, e.g., $A^0_k + A^\delta_{i|k} \in [A(v^-_{i|k}), A(v^+_{i|k})]$. To simplify notation, we introduce $A^\pm_{i|k} = A(v^\pm_{i|k})$. State uncertainty in the prediction horizon is handled by a decomposition

$$x_{i|k} = z_{i|k} + e_{i|k}, \quad z_{i|k} = \mathbb{E}_k(x_{i|k}) \tag{10}$$

where $z_{i|k}$ is the nominal prediction and $e_{i|k}$ is the uncertain component of the predicted state, which is contained within a polytopic prediction uncertainty set denoted by $\Pi_{i|k}$. The purpose of this set is to facilitate the construction of constraints that account for the uncertainty in the predictions.

The size of $\Pi_{i+1|k}$ can be reduced by defining linear feedback $Le_{i|k}$ on the preceding uncertain part of the state prediction. This makes the input predictions uncertain. The input predictions

$$u_{i|k} = c_{i|k} + Le_{i|k}, \quad i < N \tag{11}$$

are the sum of this feedback and the input degrees of freedom $c_{i|k}$, which are optimization variables that introduce feedforward into the predicted evolution of the state.

We choose L so as to attenuate the uncertainty in the prediction horizon. We define $z_{0|k}, e_{0|k}$ to be free variables in the online optimization at time step k, and constrain their sum to equal the measured state x_k. When decomposed, the uncertain dynamics (9) can be written as

$$z_{i+1|k} = A_k^0 z_{i|k} + B_k^0 c_{i|k} + w_k^0 \tag{12a}$$

$$e_{i+1|k} = A_{i|k}^{\delta} z_{i|k} + \left(A_k^0 + A_{i|k}^{\delta} + B_k^0 L + B_{i|k}^{\delta} L\right) e_{i|k} + B_{i|k}^{\delta} c_{i|k} + w_{i|k}^{\delta}. \tag{12b}$$

This decomposition is also applied to the constraints of (6), giving

$$F(z_{i|k} + e_{i|k}) + G(c_{i|k} + L e_{i|k}) \le g(\tilde{v}_k). \tag{13}$$

We define the tube cross section, $\Pi_{i|k}$, at each prediction step i, as a bounding polytope of the uncertain prediction

$$e_{i|k} \in \Pi_{i|k} = \{e : Ve \le \alpha_{i|k}\}, \quad \alpha_{i|k} \ge 0 \tag{14}$$

where $V \in \mathbb{R}^{n_V \times n_x}$ is constant and defines the directions of the facets of $\Pi_{i|k}$, while $\alpha_{i|k} \in \mathbb{R}^{n_V}$ is an optimization variable defining the scaling of each facet from the origin.

Theorem 1: If $Ve_{i|k} \le \alpha_{i|k}$, then under the dynamics of (12), $Ve_{i+1|k} \le \alpha_{i+1|k}$ if and only if there exist matrices $H_{i|k}^{+}$, $H_{i|k}^{-}$ with nonnegative elements such that

$$H_{i|k}^{\pm} V = V(A_{i|k}^{\pm} + B_{i|k}^{\pm} L) \tag{15a}$$

$$H_{i|k}^{\pm} \alpha_{i|k} + V(A_{i|k}^{\pm} z_{i|k} + B_{i|k}^{\pm} c_{i|k} + w_{i|k}^{\pm} - z_{i+1|k}) \le \alpha_{i+1|k}. \tag{15b}$$

Proof: This is a consequence of the Farkas Lemma [16]. By convexity, applying this to both extremes of the uncertainty establishes the claim of the theorem. ∎

Clearly, $H_{i|k}^{+}$ and $H_{i|k}^{-}$ depend on wind speed, so we hereby write them as $H(v_{i|k}^{\pm})$. Rather than calculating (15a) online, we find each matrix $H(v)$ corresponding to wind speeds taken from a discrete set, and introduce small conservativeness by rounding up $v_{i|k}^{+}$ and rounding down $v_{i|k}^{-}$ to select $H_{i|k}^{+}$ and $H_{i|k}^{-}$, respectively, online. The same treatment can be applied to determine necessary and sufficient conditions for (13). If $Ve_{i|k} \le \alpha_{i|k}$ for $i = 1, \ldots, N$, then (13) is satisfied if and only if there exists a matrix H_m with nonnegative elements that satisfies

$$H_m V = F + GL \tag{16a}$$

$$H_m \alpha_{i|k} + F z_{i|k} + G c_{i|k} \le g(\tilde{v}_k). \tag{16b}$$

Since the matrices $H(v)$ and H_m are designed offline so as to satisfy (15a) and (16a), there is a degree of conservativeness, and therefore to relax the constraints (15b) and (16b), which are invoked online, the degrees of freedom available in the offline design of each matrix are given up so as to minimize the sum of its elements.

V. Cost

We define $\beta_0(\tilde{v}_k)$ as the equilibrium pitch angle for the wind speed $\tilde{v}_k$. Its value is found numerically in Section VI. The target state $\bar{x}_k = [0\ 0\ \bar{\Omega}(\tilde{v}_k)^2]^T$ and target input $\bar{u}_k = [\beta_0(\tilde{v}_k)\ \bar{P}_e]^T$ are treated as time invariant, given that due to the low-pass filtering, $\tilde{v}_k$ varies sufficiently slower than the physical dynamics. We select zero cost on tower position (and hence the first element of $\bar{x}$) because the tower movement varies around an offset that varies with wind speed. As such, penalizing tower velocity is sufficient for damping, for which a zero target is appropriate. The offset element $\bar{P}_e$ is used to drive the turbine to produce as much power as possible.

We minimize the expectation of the uncertain cost of the finite horizon given by (17), where $\tilde{x}_{i|k} = x_{i|k} - \bar{x}_k$, $\tilde{u}_{i|k} = u_{i|k} - \bar{u}_k$, and $\hat{Q}$ is a terminal weighting matrix, which extends the cost to the infinite horizon. By defining a cost function that applies in both partial load and full load, and applying input constraints, the resulting controller can operate across all wind speeds for which the turbine is designed

$$J_k = \mathbb{E}\left(\tilde{x}_{N|k}^T \hat{Q} \tilde{x}_{N|k} + \sum_{i=0}^{N-1} \tilde{x}_{i|k}^T Q \tilde{x}_{i|k} + \tilde{u}_{i|k}^T R \tilde{u}_{i|k}\right). \tag{17}$$

Writing this in terms of the decision variables $c_{i|k}$ is facilitated by a lifted representation

$$\chi_{i+1|k} = \Psi_{i|k} \chi_{i|k} = \begin{bmatrix} A^0 & B^0 E & 0 & w^0 \\ 0 & M & 0 & 0 \\ A_{i|k}^{\delta} & B_{i|k}^{\delta} E & A_{i|k} + B_{i|k} L & w_{i|k}^{\delta} \\ 0 & 0 & 0 & 1 \end{bmatrix} \begin{bmatrix} z_{i|k} \\ \vec{c}_{k+i} \\ e_{i|k} \\ 1 \end{bmatrix} \tag{18}$$

where $\vec{c}_k = \left[c_{0|k}^T\ , \cdots ,\ c_{N-1|k}^T\right]^T$ and we constrain $z_{0|k} + e_{0|k} = x_k$, where x_k is known from measurement at time step k. M is the zero matrix with identity matrices on its superdiagonal blocks and $E = [I\ \ 0\ \ , \cdots ,\ \ 0]$, so that

$$M\vec{c}_k = \left[c_{1|k}^T\ , \cdots ,\ c_{N-1|k}^T\ \ 0\right]^T, \quad E\vec{c}_k = c_{0|k}. \tag{19}$$

The stage cost becomes $\mathbb{E}(\chi^T \bar{Q} \chi)$, with

$$\bar{Q} = \begin{bmatrix} Q & 0 & Q & -Q\bar{x} \\ * & E^T R E & E^T R L & -E^T R \bar{u} \\ * & * & Q + L^T R L & -L^T R \bar{u} - Q\bar{x} \\ * & * & * & \bar{x}^T Q \bar{x} + \bar{u}^T R \bar{u} \end{bmatrix} \tag{20}$$

and since $\Psi_{i|k}$ is statistically independent of $\Psi_{j|k}$ for $i \ne j$, the expectation of the products of Ψ for each prediction step can be calculated. Details are omitted for brevity [17].

VI. Control Model Identification

Numerical values for control model parameters are found in the aeroelastic simulation environment by analyzing the time series in a similar manner to [14]. The turbine in our aeroelastic code is a large rotor multimegawatt machine currently under commercial development. From (4), with appropriate simplifications, we require the following subparameters,

denoted by $FA, \beta,$ and P for fore-aft, pitch, and power, respectively

$$x_{k+1} = \left[\begin{array}{cc|c} A_{FA}(v_{i|k}) & & \begin{matrix}0\\0\end{matrix} \\ \hline 0 \quad 0 & & 1 \end{array}\right] x_k + \left[\begin{array}{c|c} B_{FA}(v_k) & \begin{matrix}0\\0\end{matrix} \\ \hline B_\beta(v_k) & B_P \end{array}\right] u_k + \left[\begin{array}{c} w_{FA}(v_k) \\ w_\beta(v_k) \end{array}\right]. \tag{21}$$

Closed-loop model identification is used, with a PI controller defining the control inputs (β, P_e) on the basis of measurements of Ω^2. Inputs to the plant can be perturbed or switched to force certain behaviors or explore larger areas of the input–output space. We use the term freezing to denote holding a control input constant to study the resulting behavior. No turbine properties are required for this model identification.

Throughout this section, we make the simplifying assumption that the identification methods will use appropriately filtered variables without separate notation. A reliable measurement of tower displacement requires a high-order low-pass filter to remove effects from blade vibration and higher order tower modes. The cutoff frequency, 4 Hz, is chosen to lie between the natural frequencies of the tower and the blades.

A. Step Response Identification

Assuming that the rotor speed varies slowly, (3) allows us to approximate the rate of change of rotor speed squared with respect to electrical power independently of wind speed. Therefore, we need only identify B_P, which is straightforward. Set the turbulence intensity in the simulation environment to 0%. Set a switch time t_s, long enough for the turbine to reach steady state, e.g., 60 s. Cause the pitch to freeze at time t_s. Cause the electrical power to step up by Δ_P from its prestep value of P_s at time t_s. Measure Δ_{Ω^2}, the change of Ω^2 per time step after the power step change. Set $B_P = \Delta_{\Omega^2}/\Delta_P$.

Finding the change in Ω^2 due to pitch is more involved, as it depends on wind speed. A separate identification for each wind speed is required to find $\hat{B}_\beta(v)$ and $\hat{w}_\beta(v)$ for each $v \in \mathcal{V}$. Functions $B_\beta(v)$ and $w_\beta(v)$ for $v \notin \mathcal{V}$ are linear interpolations of $\hat{B}_\beta(v)$ and $\hat{w}_\beta(v)$.

Our method is as follows. Set turbulence intensity to 0% and mean wind speed v. Set switch time t_s. Freeze the power at t_s. Freeze the pitch at t_s and record its value as $\beta_0(v)$. Increase the pitch by a small amount. Measure $\hat{B}_\beta(v)$, defined as the rate of change of Ω^2. Then, $\hat{w}_\beta(v) = -\beta_0 \hat{B}_\beta(v) - P_s B_P$.

B. Regression Identification

The tower dynamics model parameters are found by running simulations of 600 s and fitting a white box affine model using least squares regression. The independent values of the regression are vector time series of tower position $\mathbf{p}$, velocity $\dot{\mathbf{p}}$, and pitch angle $\mathbf{b}$. The dependent values are vector time series of tower position and velocity shifted by the MPC sample time to give two more sequences, $\mathbf{p}^+$ and $\dot{\mathbf{p}}^+$. This identification is required for each $v \in \mathcal{V}$, interpolated to give $A_{FA}(v)$, $B_{FA}(v)$, and $w_{FA}(v)$.

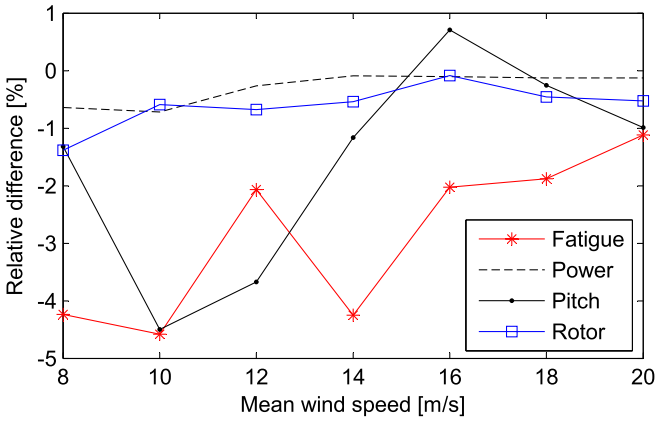

Fig. 2. Relative difference of RMPC compared with MPC for four measures across a range of mean wind speeds. Each mean wind speed has 12 runs of 600 s with different random turbulence fields. Relative difference is the measure for RMPC divided by the measure for MPC, minus one, expressed as a percentage. Fatigue is the accumulated tower base fatigue with Wöhler exponent 4. Power is the mean power output. Pitch is the total pitch travel, the sum of absolute differences in pitch in successive time steps. Rotor is the RMS rotor speed error.

Our method is as follows. Set turbulence intensity to 10% and mean wind speed v. Simulate 600 s of normal operation with a given PI controller. Set $X = [\mathbf{p} \quad \dot{\mathbf{p}} \quad \mathbf{b} \quad \mathbf{1}]$. Calculate $Y = [X^\dagger \mathbf{p}^+ \quad X^\dagger \dot{\mathbf{p}}^+]$, where $X^\dagger$ is the pseudoinverse of X corresponding to least squares regression, resulting in Y, the best fit one-step-ahead prediction model for the purpose of predicting tower dynamics. Set

$$[\hat{A}_{FA}(v) \quad \hat{B}_{FA}(v) \quad \hat{w}_{FA}(v)] = Y^T.$$

The coefficients of determination for these regressions at 12-m/s mean wind speed were 0.99 for tower displacement and 0.91 for tower velocity, implying there is more unmodeled behavior in the velocity than in the displacement.

VII. Example Results

The numerical example of this section comprises 84 aeroelastic simulations controlled with each of MPC and RMPC. The aeroelastic code is based on DTUs FLEX5, the development of which is reviewed in [18]. The simulation has 23 DoF and is sampled at 100 Hz. The MPC controllers operate sample and hold at 2 Hz and output reference pitch and power set points to dedicated pitch and power controllers that lie inside the aeroelastic code. We use a prediction horizon of $N = 8$, which at 2 Hz is longer than one tower cycle. This leads to a QP of 16 variables and 40 inequality constraints in the nominal controller and 64 variables and 226 inequality constraints in the robust controller. All inputs and outputs are scaled to operate around unity for numerical conditioning purposes. All simulations use the same parameters $N, F, G, Q, \tilde{Q},$ and R and all control model parameters. All RMPC simulations use the same parameters $V, L,$ $\tau = 0.84$ and $n_c = 2.5$.

Fatigue is measured using a rainflow count [19], as is common in the design process of wind turbines. The rainflow count raises the amplitudes of cycles in the material stress

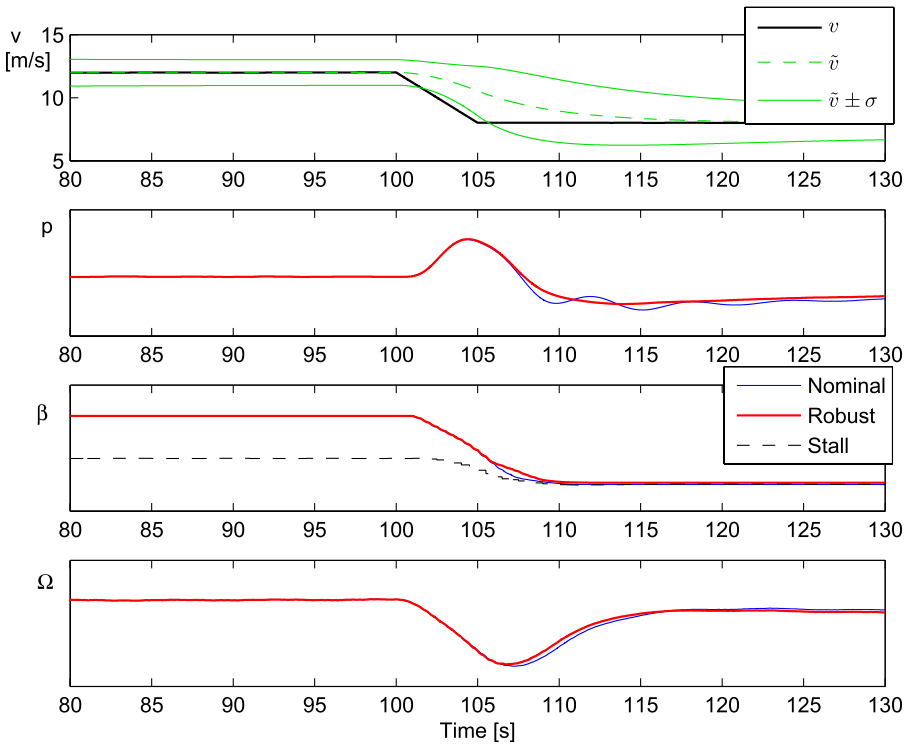

Fig. 3. Deterministic load case. Wind speed v drops from 12 to 8 m/s in 5 s. Tower displacement p is damped more using RMPC than nominal MPC. Pitch constraint is mitigated earlier, as seen in pitch β signal at 106 s. The bounds in the wind speed plot show $v^{\pm}_{i|k}$ for $n_c = 1, i \to \infty$. Axis values for tower displacement, pitch, and rotor speed Ω are omitted to protect proprietary data.

time series to the Wöhler exponent, a coefficient specific to the tower material. Twelve random wind fields are generated per mean wind speed, six at a turbulence intensity of 16% and six at 14%, as per the IEC Standard [20] higher and medium turbulence classes. Random turbulence is spatially distributed and assumes frozen turbulence, i.e., a 3-D vector field that passes through the rotor at a fixed rate determined by the mean wind speed.

Fig. 2 shows what effect robustness has on tower base fatigue, mean power, pitch travel, and rotor speed error. While the number of simulations in this trial is substantial, it is noted that accumulated fatigue estimates based on rainflow counting are sensitive to the largest peaks in the time series. A study involving more random wind fields is recommended if a high degree of statistical significance is required.

The results show that RMPC reduces tower base fatigue, pitch travel, and rotor speed error, while sacrificing a small amount of power. The effect is more pronounced at lower mean wind speeds, where the pitch constraint is active more often and the mean thrust is higher. To estimate the total reduction in fatigue that a wind turbine would receive, we use a Weibull distribution with a mean wind speed 10 m/s and a shape factor 2 as a weighting function to combine the fatigue savings across the range of mean wind speeds. This analysis shows that RMPC saves 3.2% tower base fatigue at the expense of 0.4% of power.

The benefit of RMPC is shown to be more significant at mean wind speeds where the pitch constraints are active often. The uncertainty feedback term L makes predicted inputs uncertain, which allows RMPC to anticipate input constraint activity due to potential future wind speed variations. We illustrate this effect with a deterministic load case. Fig. 3 shows the wind speed undergoing a sudden drop. Under nominal MPC, the pitch constraint saturates because $\tilde{v}$ lags v. Then, there is no pitch actuation available to dampen the tower oscillations. Under robust MPC, v lies within the uncertainty bounds of future wind speeds and predicted pitch angles hit tightened constraints earlier in time. The result is superior damping.

VIII. Conclusion

Robust MPC is compared with nominal MPC using a control model comprising three states plus scheduling parameter wind speed, without a switch from partial load to full load. The controllers operate across the whole range of wind speeds for which the turbine is designed, and are identical save for their handling of constraints.

Promising numerical results, taken from state-of-the-art load simulations representing a large rotor multimegawatt wind turbine, show that robust MPC can outperform nominal MPC, especially around nominal wind speed where the constraints are active often. Simple model identification methods are given that use only data that can be obtained from sensors available in real time on modern wind turbines.

Extensions to this brief include increasing the state space to include blade bending moments, tower side-to-side motion, and rotor azimuth and incorporation of stochastic MPC, where selected constraints can be violated with a given probability, reducing conservatism compared with RMPC.

ACKNOWLEDGMENT

The authors would like to thank Vestas for their help with the simulation environment.

REFERENCES

[1] S. Colwell and B. Basu, "Tuned liquid column dampers in offshore wind turbines for structural control," *Eng. Struct.*, vol. 31, no. 2, pp. 358–368, 2009.

[2] E. Bossanyi, "Wind turbine control for load reduction," *Wind Energy*, vol. 6, no. 3, pp. 229–244, 2003.

[3] K. Østergaard, J. Stoustrup, and P. Brath, "Linear parameter varying control of wind turbines covering both partial load and full load conditions," *Int. J. Robust Nonlinear Control*, vol. 19, no. 1, pp. 92–116, 2009.

[4] D. Mayne, J. Rawlings, C. Rao, and P. Scokaert, "Constrained model predictive control: Stability and optimality," *Automatica*, vol. 36, no. 6, pp. 789–814, 2000.

[5] N. Nanayakkara, M. Nakamura, and H. Hatazaki, "Predictive control of wind turbines in small power systems at high turbulent wind speeds," *Control Eng. Pract.*, vol. 5, no. 8, pp. 1063–1069, 1997.

[6] S. P. Kani and M. Ardehali, "Very short-term wind speed prediction: A new artificial neural network—Markov chain model," *Energy Convers. Manag.*, vol. 52, no. 1, pp. 738–745, 2011.

[7] R. Hardesty and B. Weber, "Lidar measurement of turbulence encountered by horizontal-axis wind turbine," *J. Atmos. Ocean. Technol.*, vol. 4, no. 1, pp. 191–203, 1987.

[8] A. Koerber and R. King, "Combined feedback–feedforward control of wind turbines using state-constrained model predictive control," *IEEE Trans. Control Syst. Technol.*, vol. 21, no. 4, pp. 1117–1128, Jul. 2013.

[9] A. Kumar and K. Stol, "Scheduled model predictive control of a wind turbine," in *Proc. 47th AIAA Aerosp. Sci. Meeting*, 2009, pp. 2009–2481.

[10] M. Soliman, O. Malik, and D. Westwick, "Multiple model predictive control for wind turbines with doubly fed induction generators," *IEEE Trans. Sustain. Energy*, vol. 2, no. 3, pp. 215–225, Jul. 2011.

[11] L. Henriksen, M. Hansen, and N. Poulsen, "Wind turbine control with constraint handling: A model predictive control approach," *IET Control Theory Appl.*, vol. 6, no. 11, pp. 1722–1734, 2012.

[12] M. Mirzaei, N. Poulsen, and H. Niemann, "Robust model predictive control of a wind turbine," in *Proc. Amer. Control Conf.*, 2012, pp. 4393–4398.

[13] M. Evans, M. Cannon, and B. Kouvaritakis, "Robust MPC for linear systems with bounded multiplicative uncertainty," in *Proc. IEEE 51st Annu. CDC*, Dec. 2012, pp. 248–253.

[14] A. Kusiak, Z. Song, and H. Zheng, "Anticipatory control of wind turbines with data-driven predictive models," *IEEE Trans. Energy Convers.*, vol. 24, no. 3, pp. 766–774, Sep. 2009.

[15] E. Petersen, N. Mortensen, L. Landberg, J. Højstrup, and H. Frank, "Wind power meteorology. Part I: Climate and turbulence," *Wind Energy*, vol. 1, no. 1, pp. 25–45, 1998.

[16] G. Bitsoris, "On the positive invariance of polyhedral sets for discrete-time systems," *Syst. Control Lett.*, vol. 11, no. 3, pp. 243–248, Sep. 1988.

[17] M. Cannon, B. Kouvaritakis, and X. Wu, "Probabilistic constrained MPC for multiplicative and additive stochastic uncertainty," *IEEE Trans. Autom. Control*, vol. 54, no. 7, pp. 1626–1632, Jul. 2009.

[18] P. Zhang and S. Huang, "Review of aeroelasticity for wind turbine: Current status, research focus and future perspectives," *Frontiers Energy*, vol. 5, no. 4, pp. 419–434, 2011.

[19] S. Downing and D. Socie, "Simple rainflow counting algorithms," *Int. J. Fatigue*, vol. 4, no. 1, pp. 31–40, 1982.

[20] *International Electrotechnical Committee*, IEC Standard 61400-1, 2005.